NATIONAL ADVISORY COMMITTEE FOR AERONAUTICS

WARTIME REPORT

ORIGINALLY ISSUED

October 1942 as
Memorandum Report

AERODYNAMIC CHARACTERISTICS FOR INTERNAL-BALANCE AND FRISE TYPE AILERONS ON AN NACA 6 SERIES LOW-DRAG TIP SECTION OF THE WING FOR THE XP-63 AIRPLANE

By William J. Underwood

Langley Memorial Aeronautical Laboratory
Langley Field, Va.

NACA

WASHINGTON

MEMORANDUM REPORT

for

Army Air Forces, Materiel Command

AERODYNAMIC CHARACTERISTICS FOR INTERNAL-BALANCE AND FRISE TYPE AILERONS ON AN NACA 6 SERIES LOW-DRAG TIP SECTION OF THE WING FOR THE XP-63 AIRPLANE

By William J. Underwood

INTRODUCTION

At the request of the Army Air Forces, Materiel Command, tests were made in the two-dimensional low-turbulence tunnel of a model submitted by Bell Aircraft Corporation as the tip section of the wing of the XP-63 airplane. The model was an NACA 66,2x-216 $a = 0.6$ airfoil section of 50-inch chord and made of dural according to standard sheet-metal practice. The model was fitted for an internal-balance aileron with a tab and a Frise type aileron.

Several alterations of the skirts and balance on the internal-balance aileron were tested to obtain the various aerodynamic characteristics of the aileron.

It was felt desirable to check the results from the two-dimensional low-turbulence tunnel on a smaller chord model due to the blocking effect of the large chord model at high angles of attack. The check tests were made in the two-dimensional low-turbulence pressure tunnel where more complete drag and lift results could be obtained at

approximately the same Reynolds number. The model tested in the two-dimensional low-turbulence pressure tunnel was the NACA 66,2x-116 a = 0.6 airfoil section of 24-inch chord. This model was made of laminated mahogany and was equipped with pressure orifices over the aileron. It was felt that the small change in camber between the 24-inch chord and 50-inch chord models would have no appreciable effect on the aileron characteristics.

Section lift, drag, and hinge-moment coefficients are presented herein from the results of the tests in the two-dimensional low-turbulence tunnel and the two-dimensional low-turbulence pressure tunnel.

METHOD

Lift and drag measurements for both models were made by methods described in reference 1. In the case of the NACA 66,2x-216 a = 0.6 50-inch chord model, the lift and drag coefficients were based on the nominal wing chord, c, of 50 inches, although the true chord length was 49.875 inches with the internal-balance aileron and 49.375 inches with the Frise type aileron. The hinge-moment coefficients were based on the actual dimensions of the aileron chord, c_a. The aileron configurations tested are dimensioned as a fractional part of the nominal wing chord (fig. 1). Hinge moments were measured with a torque rod hinge-moment balance. The section hinge-moment coefficient is given as

$$c_h = \frac{M}{qS_a c_a}$$

where

M hinge moment measured by angular deflection on the torque rod

q dynamic pressure $\left(\frac{1}{2}\rho V^2\right)$

S_a aileron area

c_a aileron chord

The model as delivered was equipped with a pressure seal curtain as shown in figure 1, configuration A. Rubber dam seals were installed at each end of the aileron because previous tests have shown that both the aileron balance and effectiveness are adversely affected by end flow. The models were sealed in this manner for all tests unless otherwise noted.

The aileron hinge moments on the NACA 66,2x-116 a = 0.6, 24-inch chord model were obtained from pressure-distribution measurements. The section hinge-moment coefficient is

$$c_h = c_{h_n} + c_{h_c} + c_{h_{seal}}$$

where c_{h_n} and c_{h_c} are determined by integrating the normal and chordwise pressure-distribution diagrams. The hinge moment due to the sealing curtain $c_{h_{seal}}$ is an estimate of the moment resulting from the pressure differences on the sealing curtain. This moment varies with the shape of the curtain and its position relative to the point of attachment to the aileron. For simplicity the contribution of the pressure seal curtain to the hinge moment

was assumed to be equal to that resulting from the application of a force acting perpendicular to the aileron chord at the point of attachment. This force was assumed to act at an arm of $0.53c_a$ and to be equal to $\frac{0.1\frac{1}{4}c_a}{2}(S_U-S_L)$ where S_U-S_L (reference 1) is the difference in the pressure coefficients across the sealing curtain.

RESULTS AND DISCUSSION

NACA 66,2x-216 a = 0.6 50-Inch Chord Model

Configuration A (fig. 1). - Aileron effectiveness and hinge moments for configuration A with the tab locked at zero are presented in figure 2. The hinge-moment results showed the need for more balance because the slopes of the hinge-moment-coefficient curves $\left(\frac{dc_h}{d\delta_a}\right)_{\delta_a=0}$ were too high. At high speed the stick forces would probably be too large for good maneuverability.

Configuration B (fig. 1). - Aileron effectiveness and hinge moments for configuration B are presented in figure 3. Because the slope of the hinge-moment-coefficient curve $\left(\frac{dc_h}{d\delta_a}\right)_{\delta_a=0}$ was large and because the lift coefficients actually decreased for aileron deflections greater than -12°, tests were made at only one angle of attack.

Configuration C-1 (fig. 1). - Aileron effectiveness and hinge moments for configuration C-1 with the tab locked at

zero are presented in figure 4. The corresponding drag polars are presented in figures 5(a) and 5(b). The test results were insufficient in number to determine curves. The effects of a 0.0392c tab on the effectiveness and hinge moments are presented in figures 6(a), 6(b), and 6(c). Figure 4 shows that the aileron was overbalanced for small deflections. The large rate of change in hinge moment with angle of attack $\left(\frac{dc_h}{d\alpha}\right)_{\delta_a=0}$ will cause further aileron overbalance due to rolling. The large value of $\left(\frac{dc_h}{d\alpha}\right)_{\delta_a=0}$ was attributed to the sensitivity of the pressures at slot lips, which are the same as the balance pressures, to local flow conditions in the region of the slot. The results for the aileron with the tab indicate that it may be possible to correct the overbalance by the use of a suitable tab linkage.

The effects of small leaks in the balance plate and removal of one end seal are presented in figure 7. It is seen that small leaks in the balance plate or sealing curtain do not seriously affect the hinge moment and effectiveness in the range of small deflection but have an appreciable effect at aileron deflections above 10°. The removal of one end seal, resulting in an end gap of approximately 0.375 inch, caused a large increase in the slope of the

hinge-moment-coefficient curve $\left(\frac{dc_h}{d\delta_a}\right)_{\delta_a=0}$ and an appreciable decrease in the effectiveness.

The effects of roughness on effectiveness and hinge moments are given in figures 8 and 9. In figure 8 it can be seen that roughness causes a change in $\left(\frac{dc_h}{d\delta_a}\right)_{\delta_a=0}$ and appreciably shortens the range of low hinge moments for positive deflections of the aileron.

Configuration C-2 (fig. 1). - The hinge moments for configuration C-2 are presented in figure 10. It can be seen by comparing figure 10 with figure 4 (configuration C-1) that the change in the skirt gap eliminated the aileron overbalance, and caused the rate of change of the hinge moment with angle of attack $\left(\frac{dc_h}{d\alpha}\right)_{\delta_a=0}$ to decrease. Increasing the size of the gap by shortening the skirt effectively moved the gap position forward, away from the region of rapidly changing pressures associated with the peak pressure on the aileron, and thereby reduced the sensitivity of the pressure difference across the balance portion of the aileron to changes in angle of attack and aileron deflection. Unpublished test data showed no drag increment in the low-drag range and no change in effectiveness throughout the range of aileron deflections tested due to the increase in gap size.

Configuration C-3 (fig. 1). - Hinge moments for configuration C-3 are presented in figure 11. It is seen that this skirt condition gave a still smaller rate of change of the hinge moment with angle of attack $\left(\frac{dc_h}{d\alpha}\right)_{\delta_a=0}$ than did configuration C-2 (fig. 10). Comparison of figure 11 with configuration C-2 shows that the slopes of the hinge-moment curves $\left(\frac{dc_h}{d\delta_a}\right)_{\delta_a=0}$ are about the same. Again unpublished test data showed no drag increment in the low-drag range and no change in effectiveness throughout the range of aileron deflections due to the change in the slot lip.

NACA 66,2x-116 a = 0.6 24-Inch Chord Model

The configuration tested in the two-dimensional low-turbulence pressure tunnel is given in figure 12. The results of the check test in the two-dimensional low-turbulence pressure tunnel are presented in figures 13, 14, and 15. It is seen in figure 13 that the rate of change of the hinge moment with angle of attack is of the same order as for configuration C-3 on the NACA 66,2x-216 a = 0.6 50-inch chord model. The slopes of the hinge-moment curves are for qualitative purposes only because the effect of the sealing curtain on the hinge moment could only be approximately estimated. The drag curves presented in figures 14(a) and 14(b) show a good low-drag range for the aileron

deflections tested. The dotted portion of the curves relate to the change in lift, which is attributed to sudden shift in transition to the leading edge. The lift curves for various aileron deflections are plotted against angle of attack and presented in figure 15. The same sudden shift in transition causes the flow over the aileron to separate and to show a loss in lift for a small increase in the angle of attack. This shift causes some loss in effectiveness at large aileron deflections for an angle of attack, α, of 0°, as shown in figure 13.

CONCLUSION

The results indicated that the Frise type aileron tested would not be satisfactory.

Either by increasing the size of the gap by shortening the skirt or moving the gap forward away from region of rapidly changing pressures associated with the peak pressure on the aileron, the sensitivity of the completely sealed internal-balance aileron to changes in angle of attack and aileron deflection is reduced. Because of the necessity of balancing out nearly all of the aileron hinge moment in order to obtain sufficiently light stick forces, it seems desirable to use a small balancing tab in conjunction with the internal-balance aileron, to obtain the final adjustment. If this

combination is used with configuration 0-3 (fig. 1), or one with slightly more nose balance, a reasonably satisfactory aileron should be assured.

Langley Memorial Aeronautical Laboratory,
National Advisory Committee for Aeronautics,
Langley Field, Va., October 2, 1942.

REFERENCE

1. Abbott, Ira H., von Doenhoff, Albert E., and Stivers, Louis S., Jr.: Summary of Airfoil Data. NACA ACR No. L5C05, 1945.

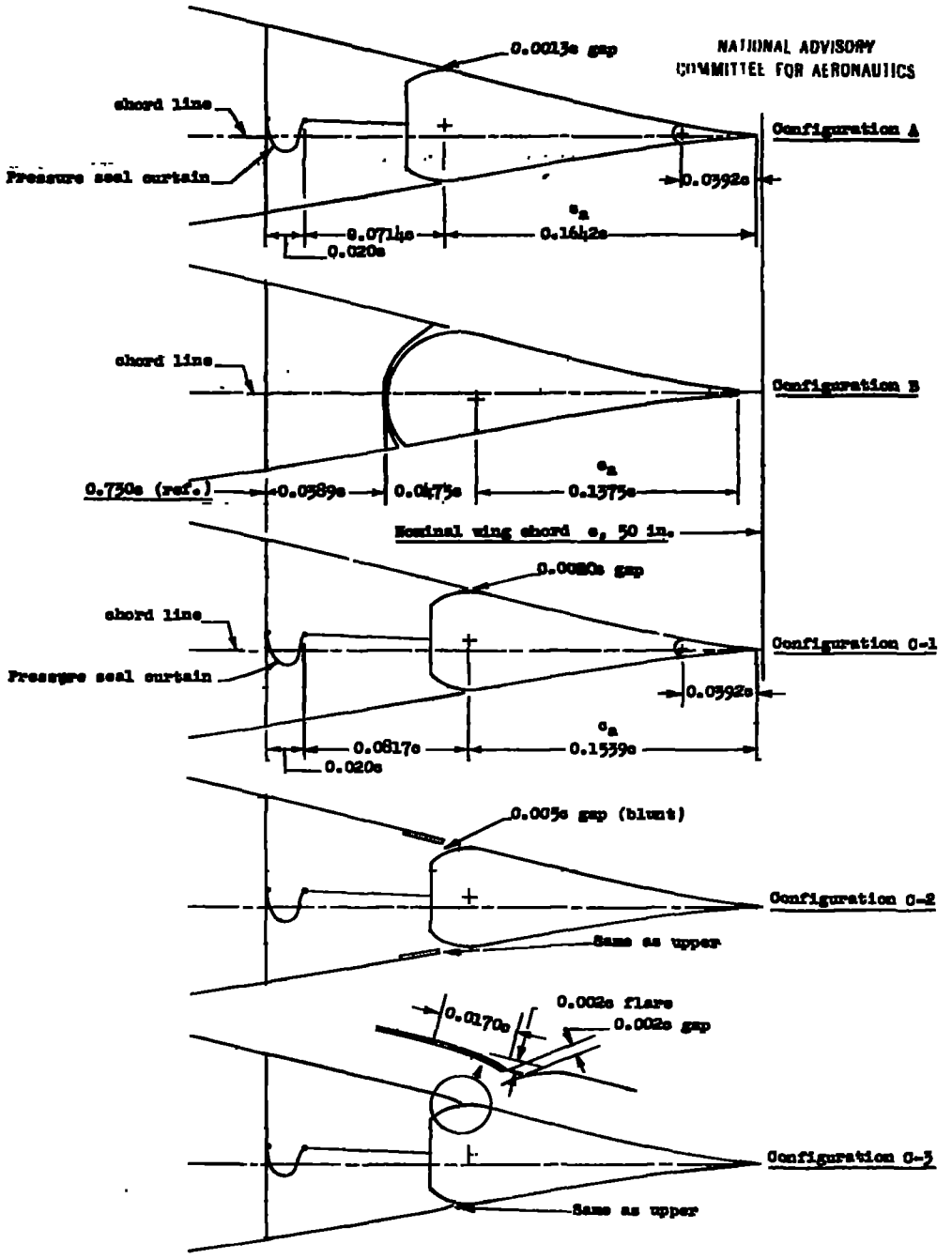

Figure 1.- Aileron configurations tested on the NACA 66,2x-216, a = 0.6, airfoil section; 50-inch chord model.

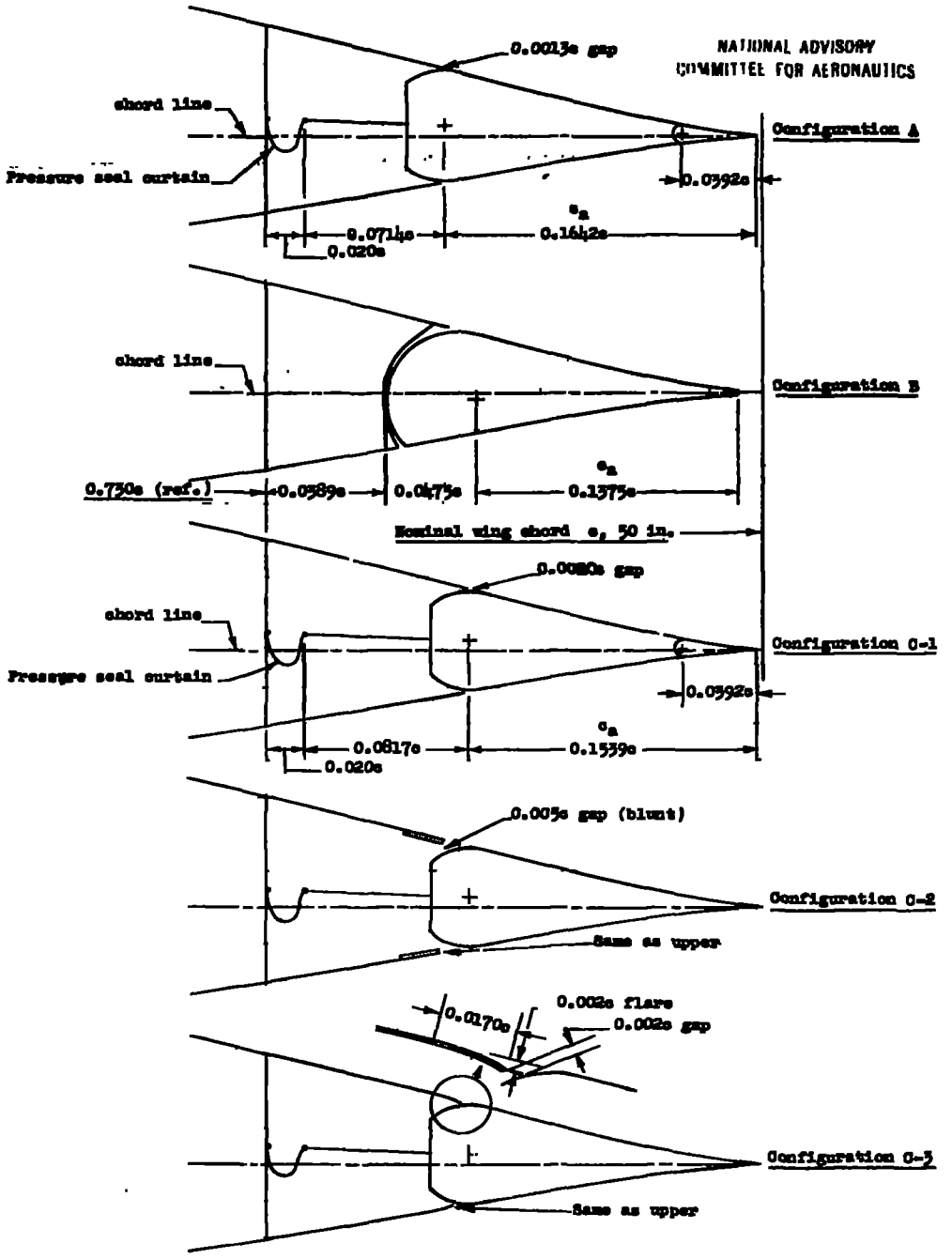

Figure 1.- Aileron configurations tested on the NACA 66,2x-216, a = 0.6, airfoil section; 50-inch chord model.

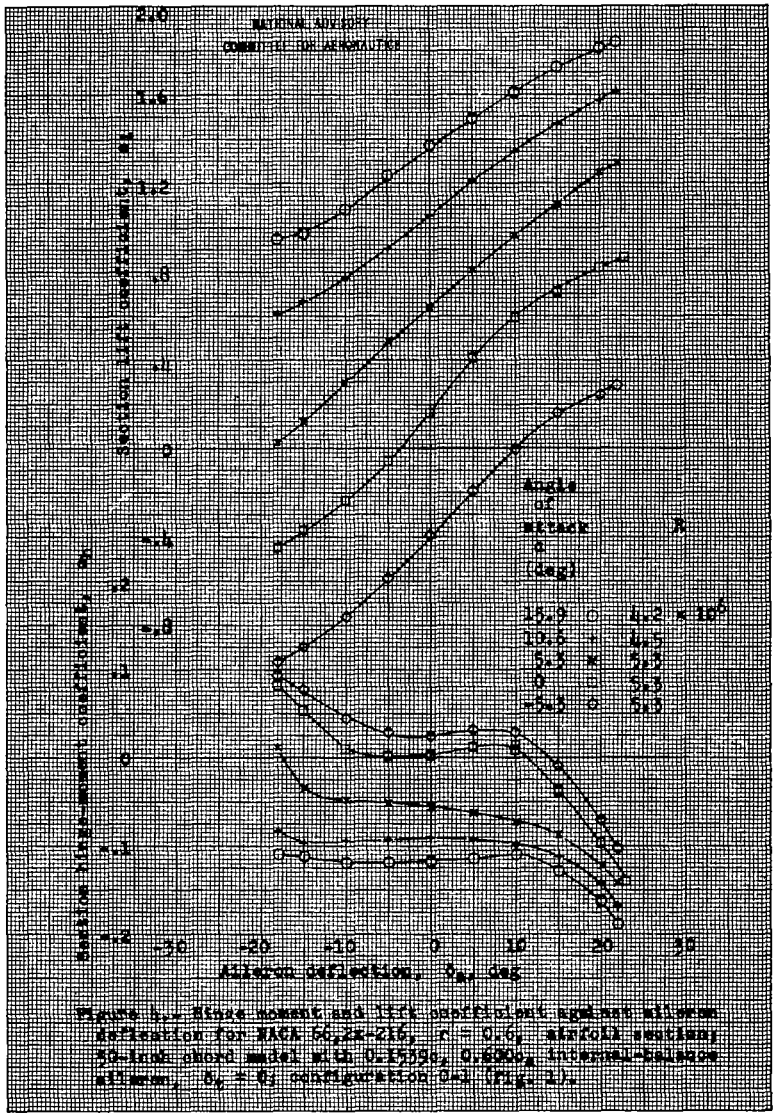

Figure 5.- Rolling moment and yaw coefficients against aileron deflection for NACA 66,2x-216, $c = 0.6$ airfoil sections; 30-inch chord model with 0.15590, 0.6000 internal-balance ailerons, $\delta_e = \delta_f$ configuration 0-1 (fig. 2).

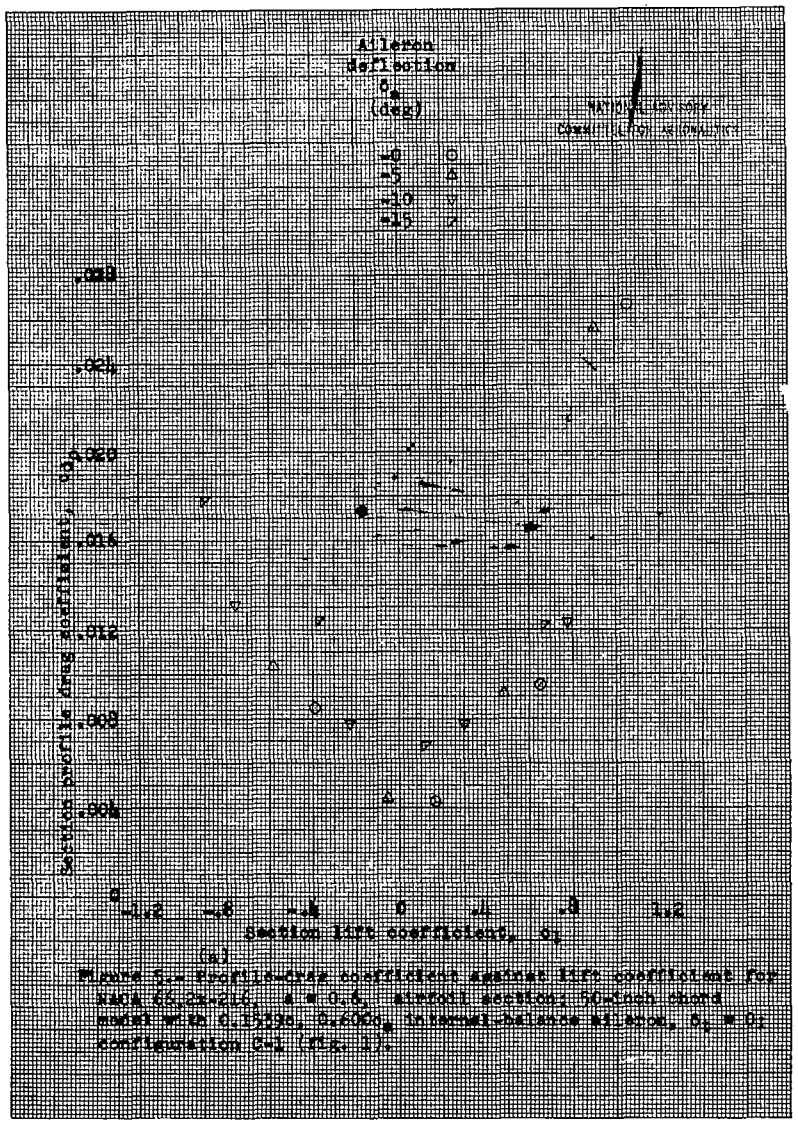

(a)

Figure 5.- Profile-drag coefficient against lift coefficient for NACA 65-206-016, $a = 0.6$, airfoil section; 50-inch chord model with 0.15c_o, 0.40c_a internal-balance aileron, $\delta_a = 0$; configuration C-1 (ref. 1).

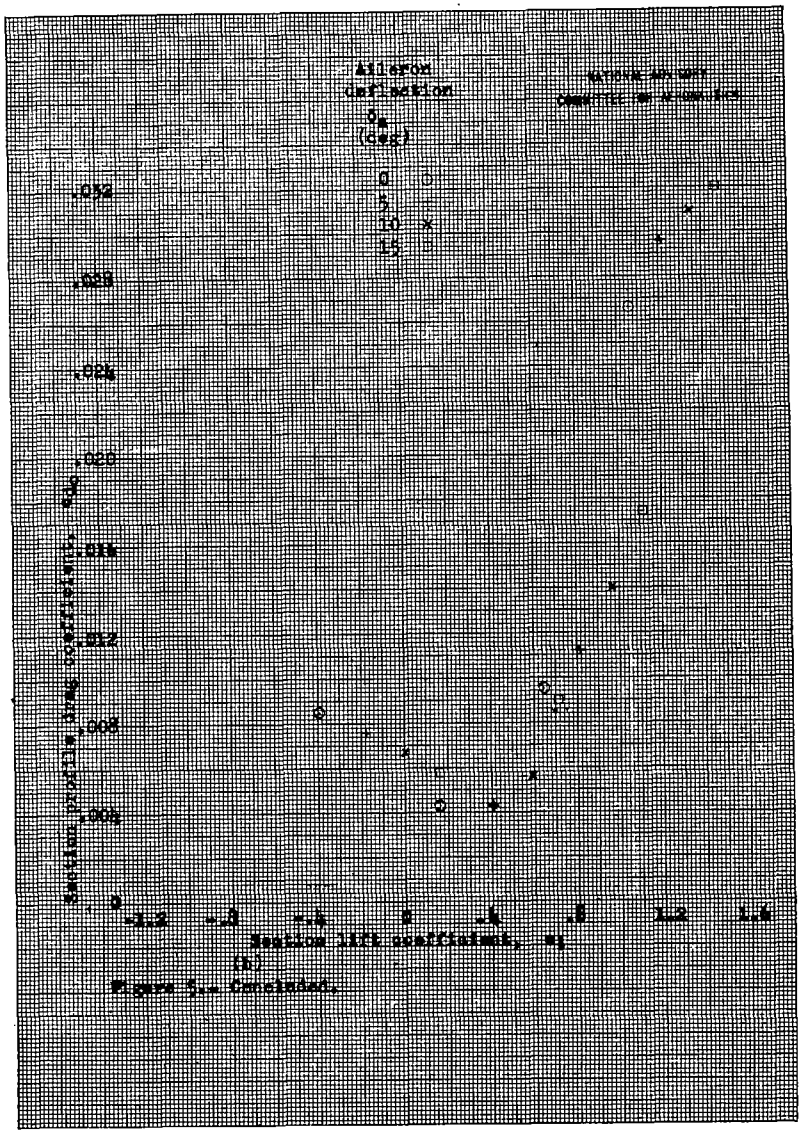

(b)

Figure 5.- Concluded.

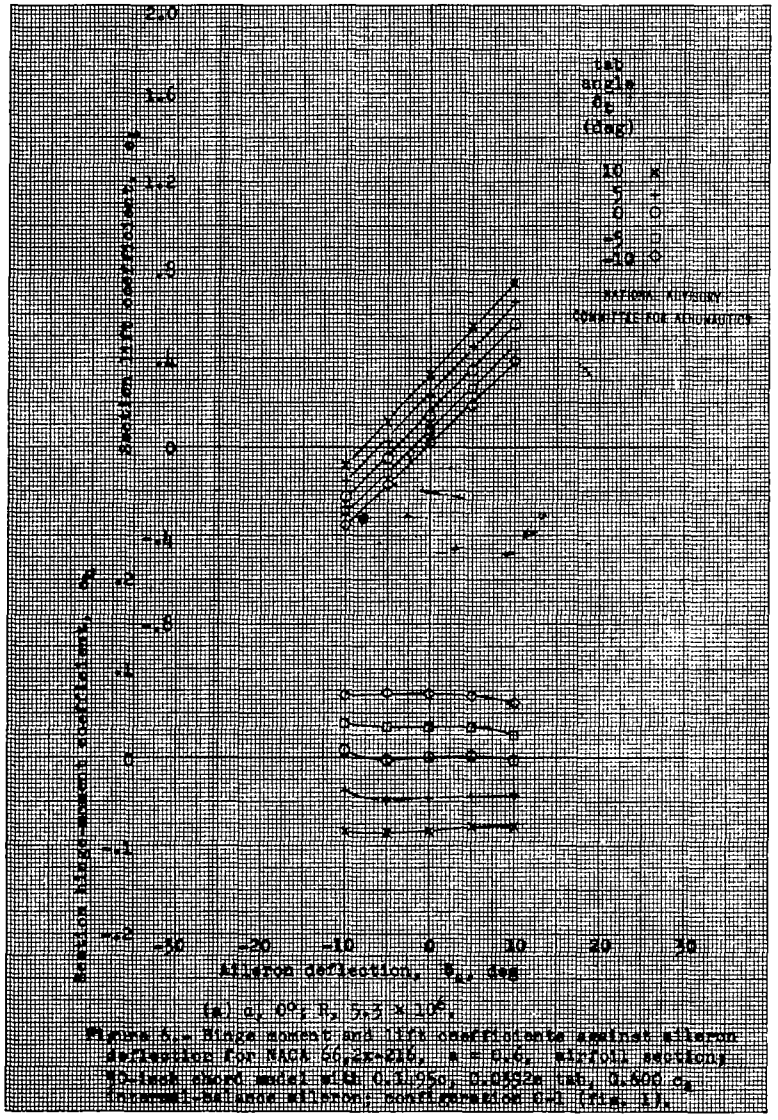

(a) α, 0°; R, 5.3×10^6.

Figure 6.- Hinge moment and lift coefficients against aileron deflection for NACA 66,2x-216, $a = 0.6$, airfoil sections; 45°-sweep wing model with 0.11050, 0.0852c tab, 0.600 c_a inboard, balance aileron; configuration 0-1 (Fig. 1).

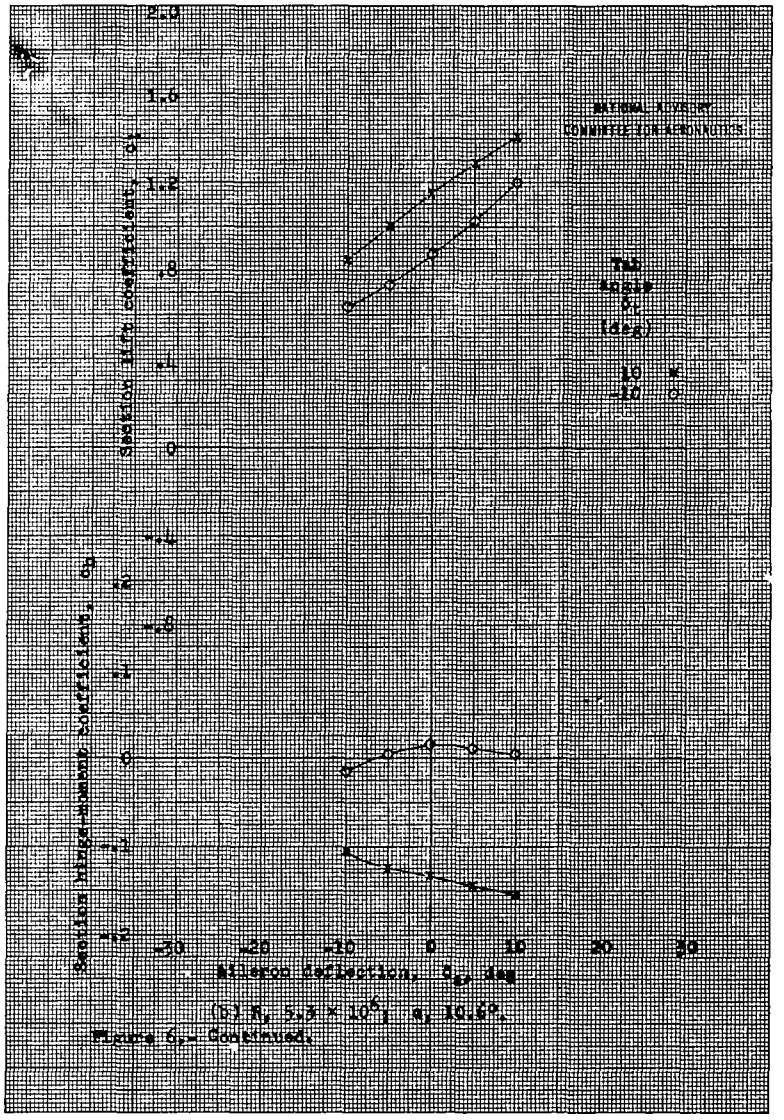

(b) R, 5.3×10^6; α, 10.6°.

Figure 6.- Continued.

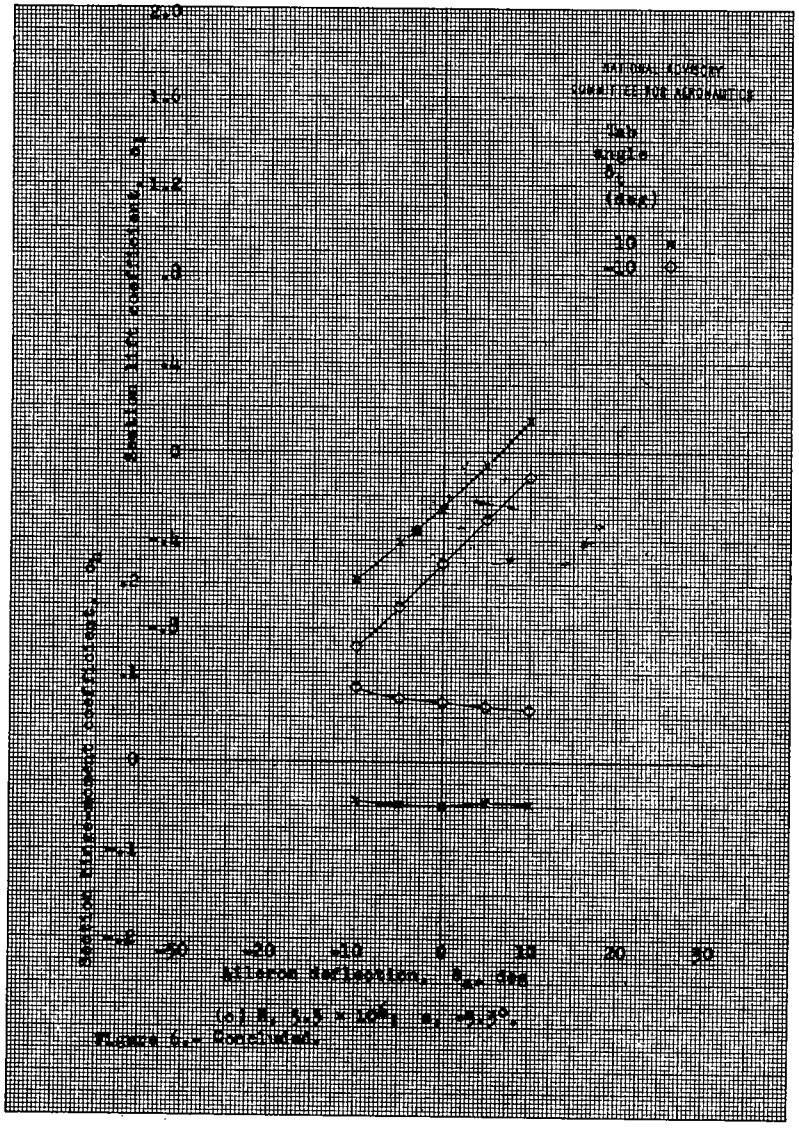

(a) R, 3.5×10^6; M, 0.25; α, 0°.

FIGURE 6.- Concluded.

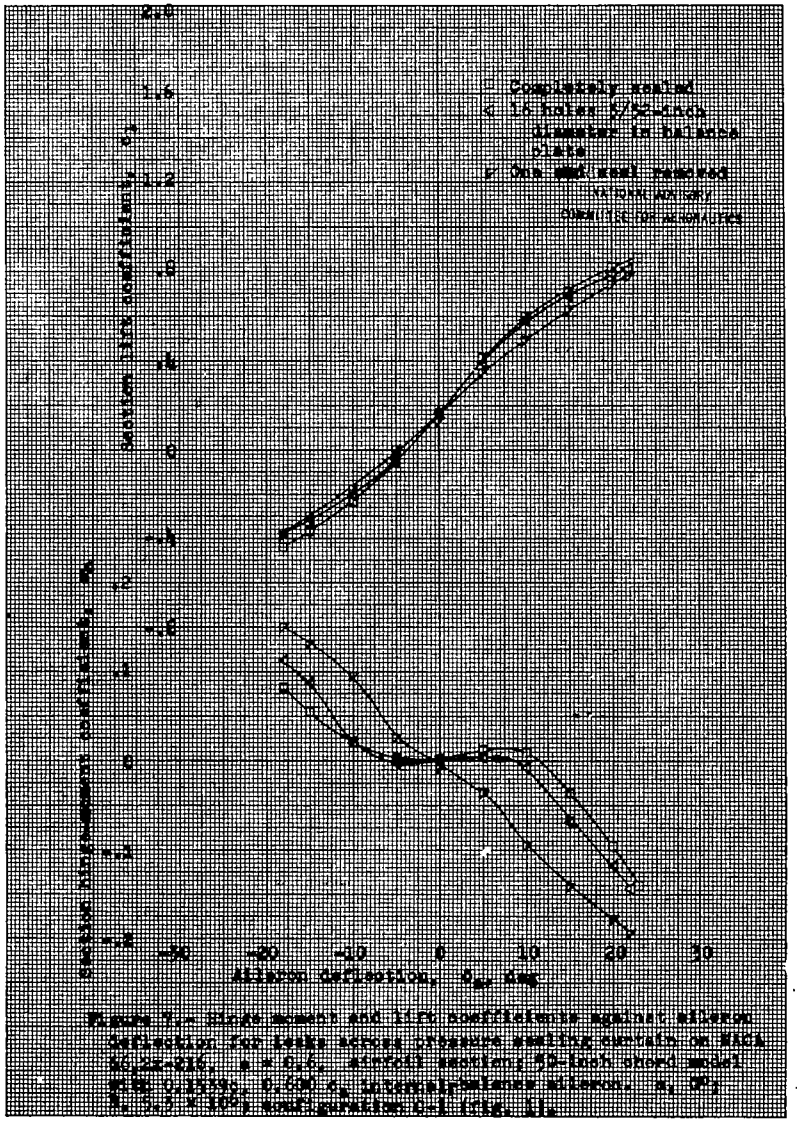

FIGURE 7.- Hinge moment and lift coefficients against aileron deflection for tests across pressure sealing curtain on NACA 66,2z-216, $a = 0.6$, airfoil sections; 50-inch chord model with 0.15c, 0.60 c internal-balance aileron. (a) R, 3.5×10^6; M, 0.25; α, 0°.

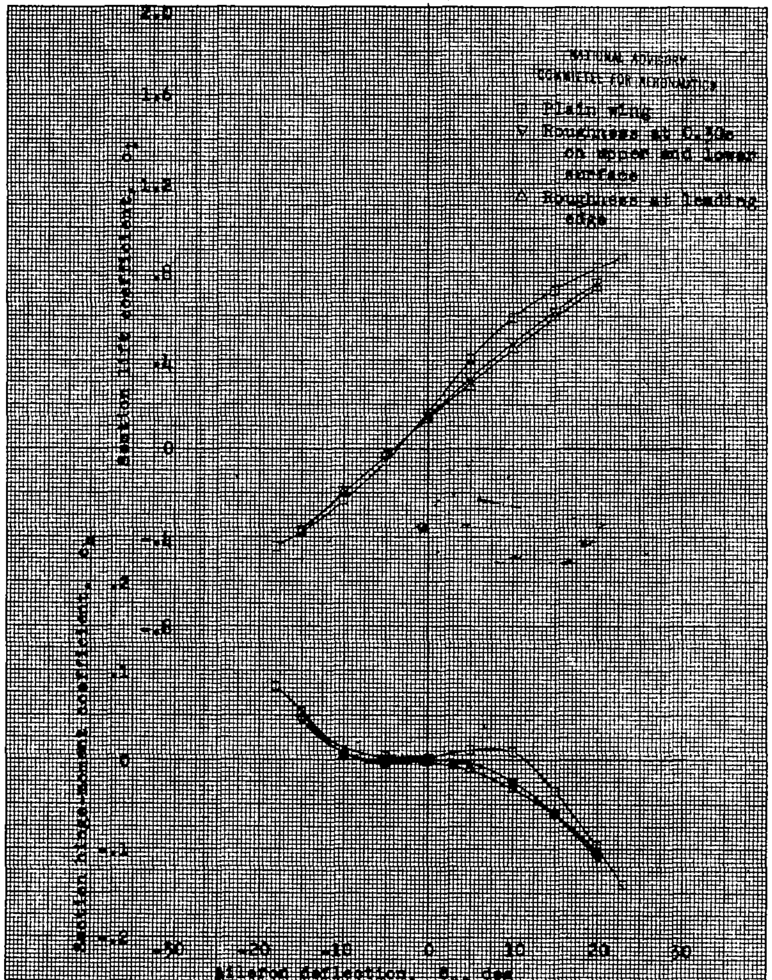

Figure 8.- Hinge moment and lift coefficients against aileron deflection with roughness on NACA 66,2x-216, a = 0.6, airfoil section; 50-inch chord model with 0.1535c, 0.600 c_a internal-balance aileron. R, 5.5×10^6; α, 0°; configuration C-1 (fig. 1).

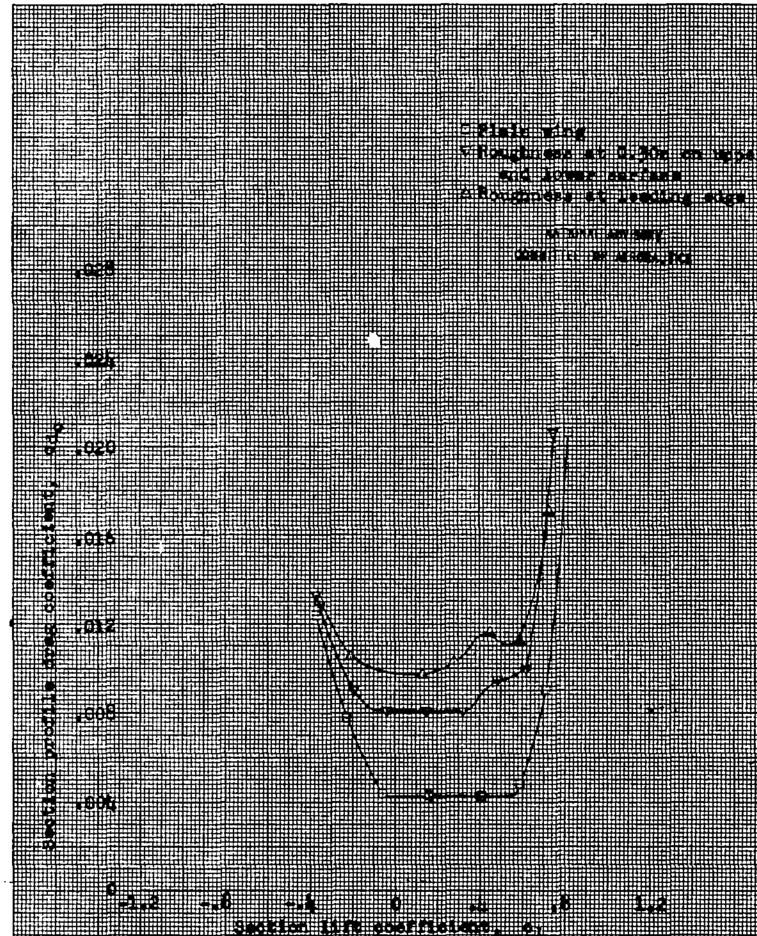

Figure 9.- Profile-drag coefficient against lift coefficient with roughness on NACA 66,2x-216, a = 0.6, airfoil section; 50-inch chord model with 0.1535c, 0.600c_a internal-balance aileron. R, 5.5×10^6; α, 0°; configuration C-1 (fig. 1).

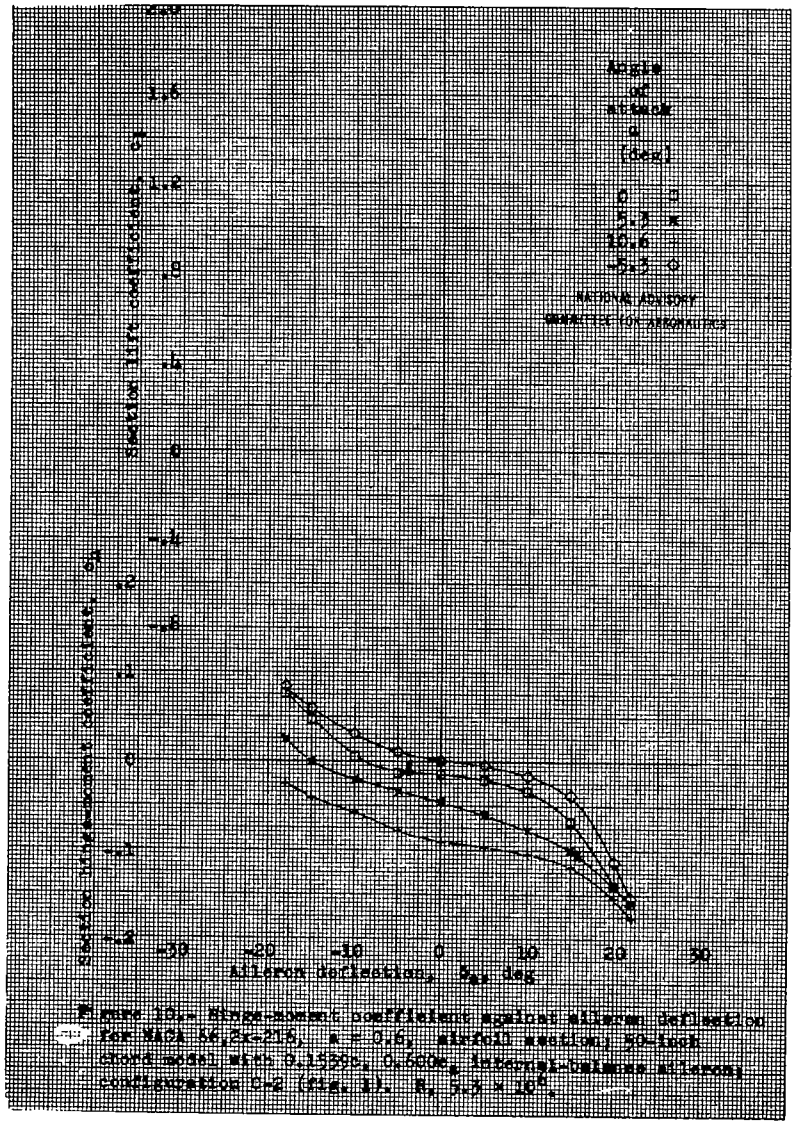

Figure 10.- Rolling-moment coefficient against aileron deflection for NACA 64,2A-216, $\kappa = 0.6$, airfoil section, 50-inch chord model with 0.1535c, 0.600s internal-balance aileron configuration C-2 (fig. 1). R, 5.3×10^6.

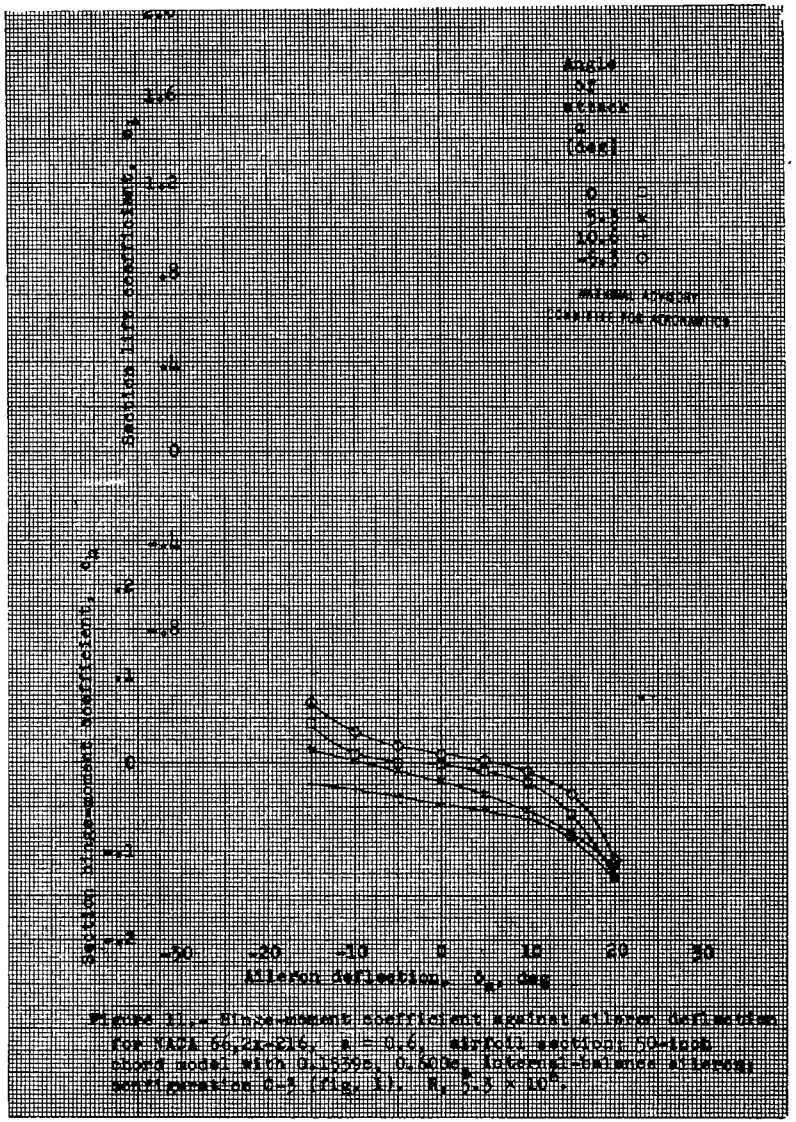

Figure 11.- Rolling-moment coefficient against aileron deflection for NACA 64,2A-216, $\kappa = 0.6$, airfoil section, 50-inch chord model with 0.1535c, 0.600s internal-balance aileron configuration C-3 (fig. 1). R, 5.3×10^6.

NATIONAL ADVISORY
COMMITTEE FOR AERONAUTICS

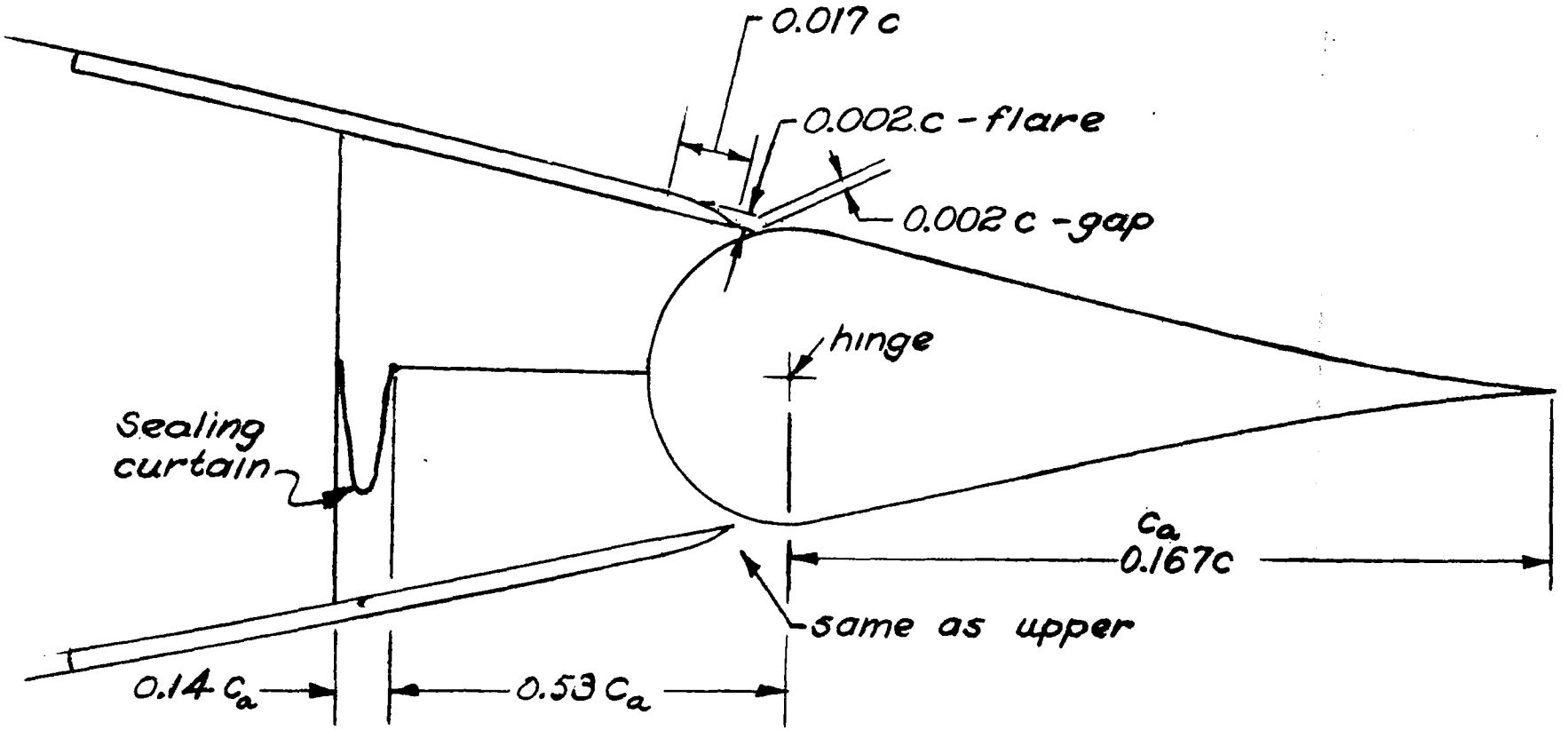

Figure 12.- Aileron configuration tested on the NACA 66,2x-116, a = 0.6, airfoil section; 24-inch chord model.

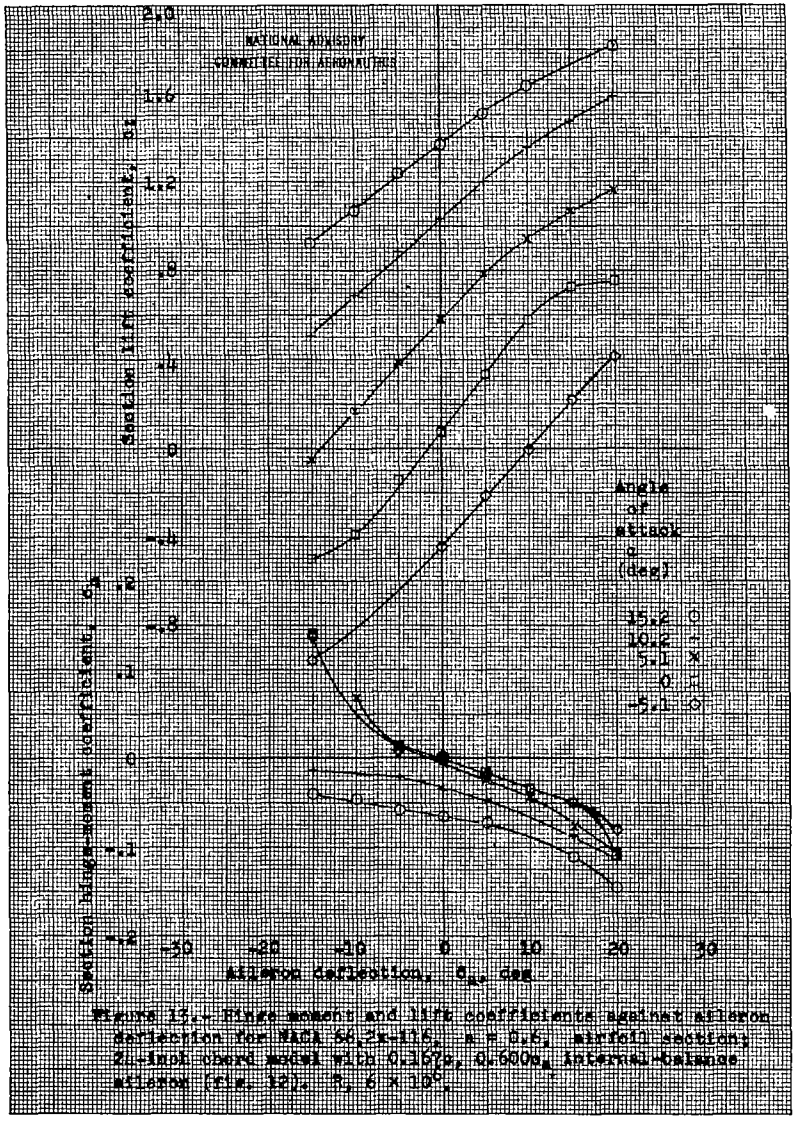

Figure 13.- Hinge moment and lift coefficients against aileron deflection for NACA 66,2x-116, $x = 0.6$, airfoil section; 2.-inch chord model with $0.167c_a$, $0.600b_a$ internal-balance aileron (fig. 12). R, 6×10^6.

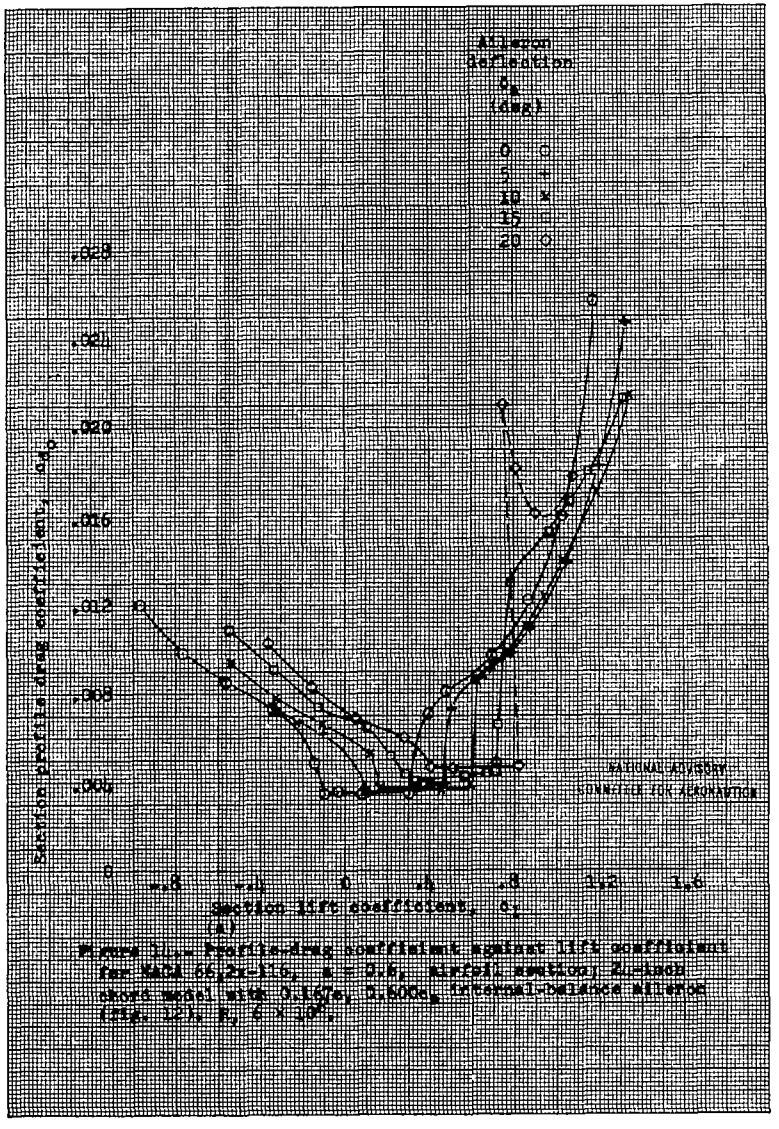

(a)

Figure 14.- Profile-drag coefficient against lift coefficient for NACA 66,2x-116, $a = 0.6$, airfoil sections; 24-inch chord model with 0.167c, 0.600b internal-balance aileron (Sta. 12); R, 6×10^6.

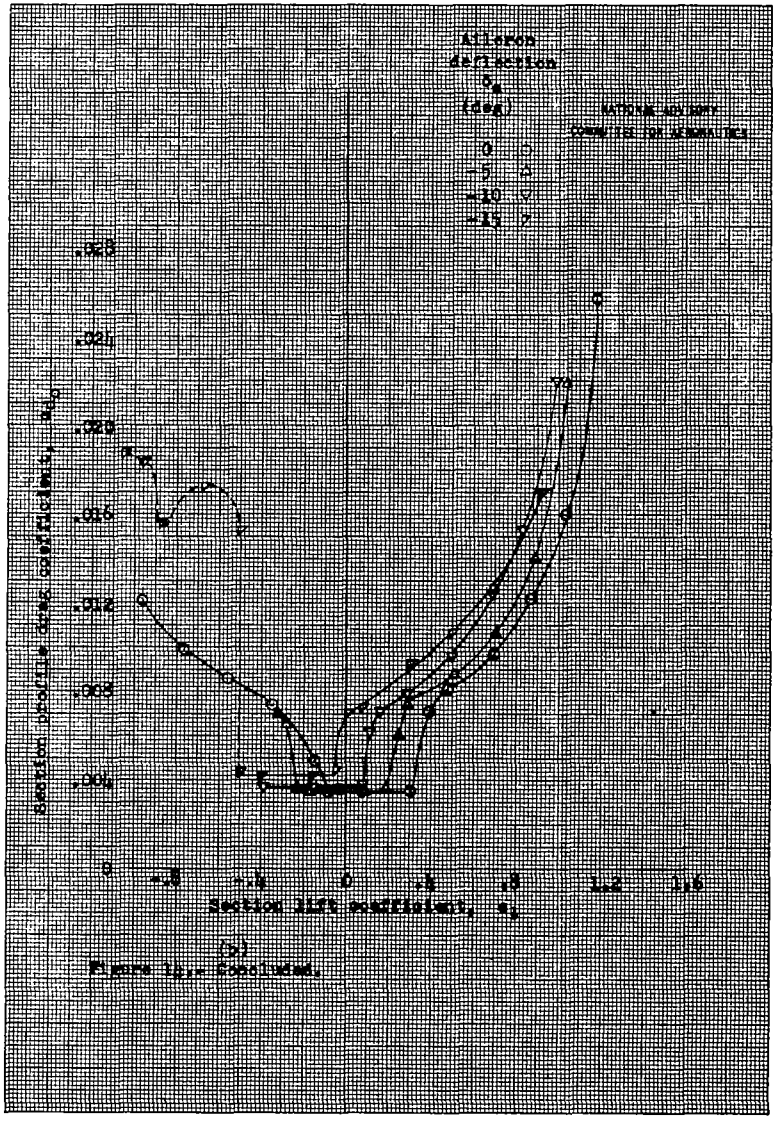

(b)

Figure 14.- Concluded.

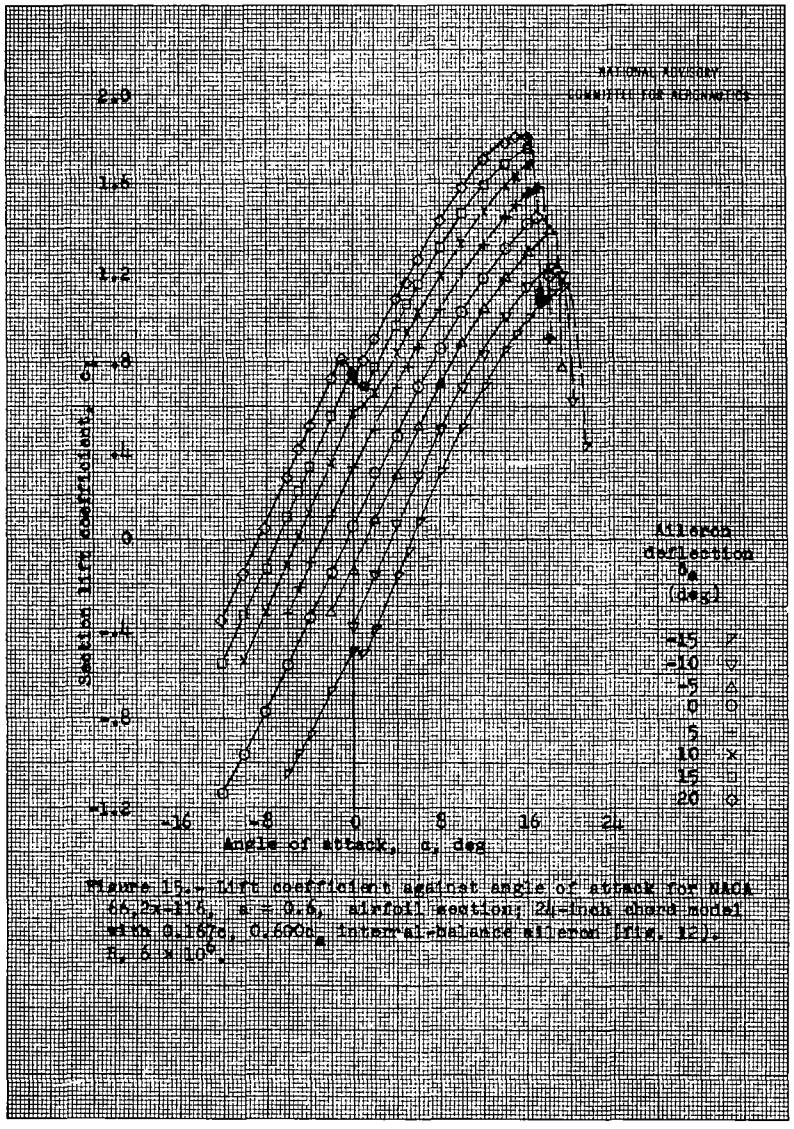

Figure 15.- Lift coefficient against angle of attack for NACA 64,2A-216, $a = 0.6$, airfoil section; 24-inch chord model with $0.167c$, $0.600c_a$ internal-balance aileron (fig. 12). R, 6×10^6.